

Theoretical Study of the Vinyl Allene Oxide to Cyclopent-2-en-1-one Rearrangement: Mechanism, Torquoselectivity and Solvent Effects

Carlos Silva López,[†] Olalla Nieto Faza,[†] Darrin M. York,[‡] and Angel R. de Lera^{*†}

Departamento de Química Orgánica, Universidade de Vigo, 36200 Vigo, Spain, and Department of Chemistry, University of Minnesota, 207 Pleasant Street SE, Minneapolis, Minnesota 55455-0431

qolera@uvigo.es

Received March 8, 2004

Density-functional calculations in the gas phase and solvent (PCM) at the B3LYP/6-311++G(3df,2p)//B3LYP/6-31++G(d,p) level were performed to study a series of six reactions that involve the rearrangement of vinyl allene oxides to cyclopent-2-en-1-ones along two distinct mechanistic pathways, namely concerted and stepwise. Calculations predict that stepwise pathways are highly competitive processes that occur via biradical/zwitterionic intermediates. Torquoselectivity is predicted to result from the concerted pathway leading to a stereodefined 4,5-disubstituted cyclopent-2-en-1-ones that should have memory of the starting terminal double-bond geometry and oxide configuration. The stepwise pathway cannot show torquoselectivity as cyclization of the planar oxidopentadienyl zwitterion can follow enantiomorphous conrotations. The concerted/stepwise mechanistic preference depends mainly on the olefin geometry and is further modulated by epoxide substitution. The influence of the solvent (PCM model for dichloromethane or water) is moderate, although the greater (de)stabilization of the polarized oxidopentadienyl zwitterions along the stepwise mechanism does alter the kinetic preferences exhibited by the systems in vacuo. Results with system **1e** suggest that, if vinyl allene oxide **II** having a double bond with *Z*-geometry, an intermediate in the biogenesis of *epi*-jasmonic acid **IV**, is processed along an *in* stepwise mechanism following ring opening, the enzyme allene oxide cyclase must enforce enantiofacial torquoselectivity.

Introduction

The highly unstable vinyl allene oxides¹ have been proposed as short-lived intermediates in the oxidative rearrangement of vinyl allenes and fulvenes to cyclopent-2-en-1-ones.^{2,3} They are also involved in the metabolism of lipids in plants and soft corals where they are formed by dehydration and rearrangement of lipid hydroperoxides. In fact, it was under physiological conditions that these fleeting intermediates could be isolated and characterized following incubation of the (13*S*)-hydroperoxides of linoleic and linolenic acids with a very active

enzyme preparation of flaxseed (*Linum usitatissimum* L.).⁴ Their rapid decomposition (chemical half-life of ca. 20 s at 0 °C and pH 7.4) afforded cyclopent-2-en-1-ones and other secondary metabolites such as α -ketols.⁴

The link between lipid hydroperoxides and cyclopent-2-en-1-ones via synthesis and rearrangement of vinyl allene oxides is now firmly established in plants.⁵ Currently, all enzymes implicated in the metabolism of the plant growth hormone *epi*-jasmonic acid **IV** have been characterized (Scheme 1), among them the allene oxide synthase⁶ and the allene oxide cyclase,⁷ responsible for the formation and rearrangement of the proposed intermediate **II** en route to *cis*-12-oxo-phytodienoic acid (PDA) **III**.⁵

The lipoxygenase pathway in invertebrates such as the soft corals also transforms arachidonic acid (AA) into metabolites with cyclopent-2-en-1-one structure.^{8–10} In contrast to the finding in plants, the allene oxide cyclase has not yet been characterized.⁵

* Corresponding author. Tel.: + (34) 986 812316. Fax: + (34) 986 812556.

[†] Universidade de Vigo.

[‡] University of Minnesota.

(1) Chan, T. H. *Tetrahedron* **1980**, *36*, 2269.

(2) (a) Grimaldi, J.; Bertrand, M. *Tetrahedron Lett.* **1969**, 3269. (b) Bertrand, M.; Dulcere, J. P.; Gil, G. *Tetrahedron Lett.* **1977**, 4403. (c) Malacria, M.; Roumestant, M. L. *Tetrahedron* **1977**, *33*, 2813. (d) Doutheau, A.; Goré, J.; Malacria, M. *Tetrahedron* **1977**, *33*, 2393. (e) Doutheau, A.; Sartoretti, J.; Goré, J. *Tetrahedron* **1983**, *39*, 3059. (f) Doutheau, A.; Goré, J.; Diab, J. *Tetrahedron* **1985**, *41*, 329. The acetoxymercuration and acetoxythallation of vinyl allenes can also be considered to follow a similar mechanism: (g) Delbecq, F.; Goré, J. *Tetrahedron Lett.* **1976**, 3459. (h) Baudouy, R.; Delbecq, F.; Goré, J. *Tetrahedron* **1980**, *36*, 189. (i) Baudouy, R.; Sartoretti, J.; Choplin, F. *Tetrahedron* **1983**, *39*, 3293. The photooxidation of vinylallenes also leads to cyclopentenones: (j) Malacria, M.; Goré, J. *J. Org. Chem.* **1979**, *44*, 885.

(3) Kim, S. J.; Cha, J. K. *Tetrahedron Lett.* **1988**, *29*, 5613. For the decomposition of fulvene hydroperoxides, see: Erden, I.; Xu, F.-P.; Drummond, J.; Alstad, R. *J. Org. Chem.* **1993**, *58*, 3611.

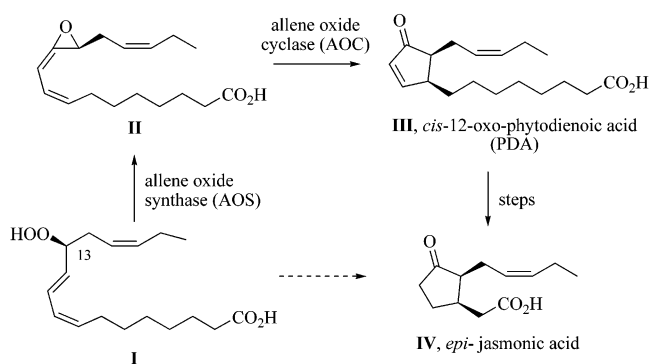
(4) (a) Baertschi, S. W.; Brash, A. R.; Harris, T. M. *J. Am. Chem. Soc.* **1989**, *111*, 5003. (b) Brash, A. R.; Baertschi, S. W.; Ingram, C. D.; Harris, T. M. *J. Proc. Natl. Acad. Sci. U.S.A.* **1988**, *85*, 3382.

(5) Tijet, N.; Brash, A. R. *Prostaglandins and Other Lipid Mediators* **2002**, 68–69, 423.

(6) (a) Song, W.-C.; Brash, A. R. *Science* **1991**, *253*, 781. (b) Boutaud, O.; Brash, A. R. *J. Biol. Chem.* **1999**, *274*, 33764.

(7) Ziegler, J.; Stenzel, I.; Hause, B.; Maucher, H.; Hamberg, M.; Grimm, R.; Ganai, M.; Wasternack, C. *J. Biol. Chem.* **2000**, *275*, 19132.

SCHEME 1



In the absence of tridimensional structures,¹¹ the mechanistic details of the lipoxygenase-mediated pathway to cyclopent-2-en-1-one natural products remain purely speculative. An attempt to gain theoretical insight into the rearrangement of parent vinyl allene oxide to cyclopent-2-en-1-one has been recently reported at the 6-31G(d) level¹² using DFT methods¹³ with Becke's three-parameter functional¹⁴ (U)B3LYP.¹⁵ For the rearrangement of the parent vinyl allene oxide **1a** and *Z*-propenyl oxide **1b** (Scheme 2), Hess and co-workers found diverging and competing mechanistic pathways. The first mechanism (**a** in Scheme 2) was described as a concerted rearrangement of the *s-cis* conformer of the reactant (**3a**)

(8) For biomimetic studies, see: (a) Corey, E. J.; d'Alarcao, M.; Matsuda, S. P. T.; Lansbury, P. T.; Yamada, Y. *J. Am. Chem. Soc.* **1987**, *109*, 289. (b) Corey, E. J.; Ritter, K.; Yus, M.; Nájera, C. *Tetrahedron Lett.* **1987**, *28*, 3547. (c) Corey, E. J.; Matsuda, S. P. T. *Tetrahedron Lett.* **1987**, *28*, 4247.

(9) The early suggestion that the pharmaceutically important prostaglandins (PGA₂ methyl ester acetate) also followed a lipoxygenase pathway in soft corals (in contrast to the endoperoxide pathway in mammals) through vinylallene oxides appears now unlikely. After years of controversy, it has been established that the prostaglandins in corals are synthesized by the cyclooxygenase pathway^{10, 11} without involvement of allene oxides as intermediates.

(10) Varvas, K.; Järving, I.; Koljak, R.; Valmsen, K.; Brash, A. R.; Samel, N. *J. Biol. Chem.* **1999**, *274*, 9923.

(11) Crystal structures of several cyclooxygenases from different species in the presence of substrate (AA) or product (PGG₂) have yielded valuable insights into the structural factors governing the efficient creation of the bicyclic endoperoxide ring and five chiral centers of PGG₂ from the achiral precursor AA, the first committed step of the biosynthetic path. (a) Kiefer, J. R.; Pawlitz, J. L.; Moreland, K. T.; Stegeman, R. A.; Hood, W. F.; Gierse, J. K.; Stevens, A. M.; Goodwin, D. C.; Rowlinson, S. W.; Marnett, L. J.; Stallings, W. C.; Kurumbail, R. G. *Nature* **2000**, *405*, 97. (b) Malkowski, M. G.; Ginell, S. L.; Smith, W. L.; Garavito, R. M. *Science* **2000**, *289*, 1933. (c) Thuresson, E. D.; Lakkides, K. M.; Rieke, C. J.; Sun, Y.; Wingerd, B. A.; Micielli, R.; Mulichak, A. M.; Malkowski, M. G.; Garavito, R. M.; Smith, W. L. *J. Biol. Chem.* **2001**, *276*, 10347. (d) Thuresson, E. D.; Malkowski, M. G.; Lakkides, K. M.; Rieke, C. J.; Mulichak, A. M.; Ginell, S. L.; Garavito, R. M.; Smith, W. L. *J. Biol. Chem.* **2001**, *276*, 10358. (e) Malkowski, M. G.; Thuresson, E. D.; Lakkides, K. M.; Rieke, C. J.; Micielli, R.; Smith, W. L.; Garavito, R. M. *J. Biol. Chem.* **2001**, *276*, 37547.

(12) Hess, B. A., Jr.; Smentek, L.; Brash, A. R.; Cha, J. K. *J. Am. Chem. Soc.* **1999**, *121*, 5603.

(13) (a) Parr, R. G.; Yang, W. *Density Functional Theory of Atoms and Molecules*; Oxford: New York, 1989. (b) Ziegler, T. *Chem. Rev.* **1991**, *91*, 651. (c) Lee, C.; Yang, W.; Parr, R. G. *Phys. Rev. B* **1988**, *37*, 785. (d) For a description of density functionals as implemented in the Gaussian series of programs, see: Johnson, B. G.; Gill, P. M. W.; Pople, J. A. *J. Chem. Phys.* **1993**, *98*, 5612.

(14) (a) Becke, A. D. *Phys. Rev. A* **1988**, *38*, 3098. (b) Becke, A. D. *J. Chem. Phys.* **1993**, *98*, 5648.

(15) Preliminary studies had shown that DFT methods were appropriate for the treatment of zwitterionic or diradical intermediates, which are conceivably formed along the pathways from allene oxide to cyclopropanone: Hess, B. A., Jr.; Eckart, U.; Fabian, J. *J. Am. Chem. Soc.* **1998**, *119*, 12310.

to cyclopent-2-en-1-one **5a**, and the transition structure **4a** showed features of an S_N2 reaction. In the second mechanism (Scheme 2, **b**), the bond-formation step was a conrotatory electrocyclic ring closure of an oxidopentadienyl zwitterion **9a** (the zwitterionic analogue of a Nazarov-type intermediate).¹⁶ However, the rate-limiting step of this stepwise process was found earlier in the reaction coordinate and corresponds to the opening of the epoxide ring of *s-trans-1a* to afford **7a** via TS **6a**. TS **8a** connects the starting *s-trans-7a* (sickle form) with the *s-cis-9a* (U form) conformers of the oxidopentadienyl zwitterion and has the vinyl group orthogonal to the oxyallyl function. The difference in activation energies between both mechanisms available to the unsubstituted vinyl allene oxide **1a** was sufficient (2.7 kcal/mol) to drive the rearrangement along the concerted path.¹²

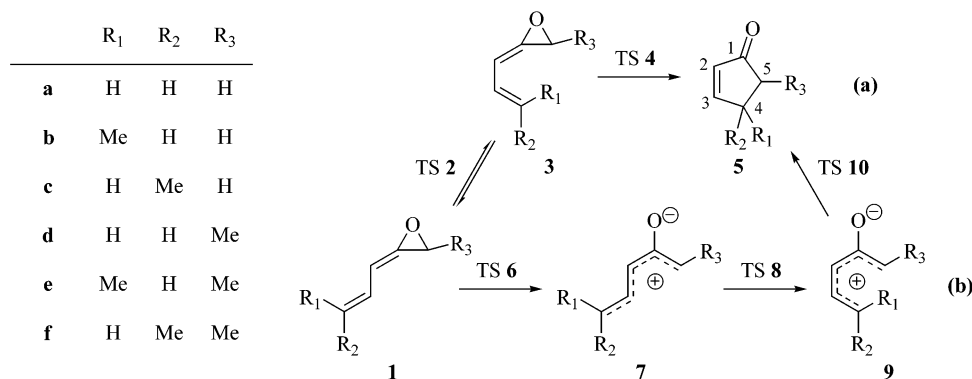
At the 6-31G(d) level of theory, similar activation energies for the stepwise rate-limiting transition state of **1a** and **1b** were computed (ca. 27.0 kcal/mol). But steric effects in **1b** clearly shifted the concerted transition state 5 kcal/mol away from the reactants (30.16 kcal/mol). This was an initial evidence of how acute the steric effects can be in the cyclization for the gas-phase competing pathways during the rearrangement of *Z*-propenyl allene oxide **1b** to 4-methylcyclopent-2-en-1-one **5b**. This mechanistic dichotomy with an energy balance critically sensitive to the presence of substituents on the reactant led Hess and co-workers to suggest that concerted and stepwise pathways might also enter into competition in the biosynthesis of natural cyclopentenones such as those depicted in Scheme 1 from vinyl allene oxides with *Z*-geometry of the terminal double bond.¹²

The work of Hess et al. was intriguing, but left open the question as to the steric course of the rearrangement, which was not fully considered, and the effect of solvation on the reaction that was neglected in their calculations. The stereochemical issues in the biogenesis of **IV** from **I** are clearly more complex than those briefly considered in the preliminary study of the *Z*-propenyl allene oxide rearrangement (**1b** → **5b**).¹² Being substituted at both terminal carbons, vinyl allene oxide **II** translate with high fidelity these stereogenic units into the vicinal chiral centers of the rearrangement product **III**. A comprehensive stereochemical analysis of the mechanistic path can shed additional light into the extent of competition between concerted and stepwise processes both in simple alkenyl allene oxides and in the more complex biological substrates. Torquoselectivity¹⁷ is the term coined by Houk to describe the stereoselectivity in electrocyclic ring opening reactions due to the preference for one of the orbital symmetry allowed conrotatory or disrotatory motions of the cyclizing termini. The term, although restrictive in its definition, could also be extended appropriately to other concerted reactions involving closure

(16) For reviews, see: (a) Denmark, S. E. Nazarov and Related Cationic Cyclizations. In *Comprehensive Organic Synthesis*, Vol. 5; Trost, B. M., Fleming, I., Paquette, L. A., Eds.; Pergamon Press: Oxford, 1991; Vol. 5, pp 751–784. (b) Habermas, K. L.; Denmark, S. E.; Jones, T. K. The Nazarov Cyclization. In *Organic Reactions*; Paquette, L. A., Ed.; Wiley: New York, 1994; Vol. 45, pp 1–158.

(17) (a) Houk, K. N. Stereoselective Electrocyclizations and Sigma-tropic Shifts of Strained Rings: Torquoelectronics. In *Strain and Its Implications in Organic Chemistry*; de Meijere, A., Blechert, S., Eds.; Kluwer Academic Publishers: Dordrecht, 1989; pp 25–37. (b) Dolbier, W. R.; Koroniak, H.; Houk, K. N.; Sheu, C. *Acc. Chem. Res.* **1996**, *29*, 471.

SCHEME 2



or opening of rings that translate stereochemical information from the reactants to the products. A fundamental understanding of the nature of substituent effects on the torquoselectivity of vinyl allene oxide rearrangements could be gleaned from theoretical investigation of a series of compounds with varying stereogenic units at the cyclizing termini.

In addition, the stepwise process was expected to be more sensitive to solvent effects, given the zwitterionic nature of the intermediates along the pathway, and changes in the mechanistic preferences were considered feasible in the presence of solvent relative to those predicted by the computations in vacuo.

We report a detailed theoretical study of the rearrangement of a series of vinyl allene oxides **1a–f** (Scheme 2) in the gas phase and in aqueous solution and organic (dichloromethane) solvent. The free energy profiles for each reaction along with the structures at each stationary point in the reaction path are characterized. The solvent and substituent factors that govern torquoselectivity and kinetically favorable rearrangement pathways are assessed, and the chemical and biological implications of these results are discussed.

Computational Methods

All geometry optimizations in this study have been performed using the Gaussian 98¹⁸ suite of programs. They were performed using the three-parameter exchange functional of Becke¹⁴ in conjunction with the gradient corrected correlation functional of Lee, Yang, and Parr.^{13c} Geometry optimizations and analytic frequency calculations were performed with the 6-31++G(d,p) basis set, followed by single-point energy refinement with the 6-311++G(3df,2p) basis set. This protocol is designated B3LYP/6-311++G(3df,2p)//6-31++G(d,p). This basis set used in the present work is slightly larger than that used for geometries and frequencies in the G2 method¹⁹ that typically yield atomization energies, ionization energies and

relative energies within ~1 kcal/mol of experimental values. The use of diffuse functions was deemed prudent based on preliminary results that indicated some of the structures present regions of localized negative charge and the fact that some of them also tend to converge toward unstable wave functions. The choice of density functional theory (DFT)¹³ to include electron correlation at a reasonable computational cost was based on precedents that show DFT provides a reliable description of zwitterionic or diradical species,¹⁵ as well as transition structures of pericyclic reactions.²⁰ Becke's three-parameter exchange functional¹⁴ with the nonlocal correlation functional of Lee, Yang and Parr^{13c} (B3LYP) was used to compute the geometries, energies and normal-mode vibrational frequencies of the reactants, the corresponding transition structures and the products. For each optimized transition structure, only one imaginary frequency was found in the diagonalized mass-weighted Hessian matrix, and the corresponding vibrational mode was confirmed to be associated with nuclear motion along the reaction coordinate under study. In several significant cases intrinsic reaction coordinates (IRC)²¹ calculations were performed to determine an unambiguous path that connect transition structures with reactant and products. Bond orders and atomic charges were calculated with the natural bond orbital (NBO)²² method. Nucleus independent chemical shifts (NICS)²³ were calculated by means of the gauge-independent atomic orbitals²⁴ (GIAO) method. Single-point solvation calculations were performed at the optimized geometries using the polarizable continuum model (PCM)²⁵ using UAHF radii²⁶ and a variation of the conductor-like screening model (COSMO)²⁷ as implemented in Gaussian 98.

Single-point CASSCF (the full optimized reaction space type) calculations with the 6-311++G(d,p) basis set have been performed for transition state **10a** with the GAMESS²⁸ pack-

(18) Gaussian 98 (Revision A.1.1). Frisch, M. J.; Trucks, G. W.; Schlegel, H. B.; Scuseria, M. A.; Robb, M. A.; Cheeseman, J. R.; Zakrzewski, V. G.; Montgomery, J. A.; Stratmann, R. E.; Burant, J. C.; Dapprich, S.; Millam, J. M.; Daniels, A. D.; Kudin, K. N.; Strain, M. C.; Farkas, O.; Tomasi, J.; Barone, V.; Cossi, M.; Cammi, R.; Mennucci, B.; Pomelli, C.; Adamo, C.; Clifford, S.; Ochterski, J.; Petersson, G. A.; Ayala, P. Y.; Cui, Q.; Morokuma, K.; Salvador, P.; Dannenberg, J. J.; Malick, D. K.; Rabuck, A. D.; Raghavachari, K.; Foresman, J. B.; Cioslowski, J.; Ortiz, J. V.; Baboul, A. G.; Stefanov, B. B.; Liu, G.; Liashenko, A.; Piskorz, P.; Komaromi, I.; Gomperts, R.; Martin, R. L.; Fox, D. J.; Keith, T.; Al-Laham, M. A.; Peng, C. Y.; Nanayakkara, A.; Challacombe, M.; Gill, P. M. W.; Johnson, B.; Chen, W.; Wong, M. W.; Andres, J. L.; Gonzalez, C.; Head-Gordon, M.; Replogle, E. S.; Pople, J. A. Gaussian, Inc., Pittsburgh, PA, 2001.

(19) (a) Curtiss, L. A.; Jones, C.; Trucks, G. W.; Raghavachari, K.; Pople, J. A. *J. Chem. Phys.* **1990**, *93*, 2537 (b) Curtiss, L. A.; Carpenter, J. E.; Raghavachari, K.; Pople, J. A. *J. Chem. Phys.* **1992**, *96*, 9030.

(20) Goldstein, E.; Beno, B.; Houk, K. N. *J. Am. Chem. Soc.* **1996**, *118*, 6036.

(21) (a) González, C.; Schlegel, H. B. *J. Phys. Chem.* **1989**, *90*, 2154. (b) González, C.; Schlegel, H. B. *J. Phys. Chem.* **1990**, *94*, 5523.

(22) Glendening, E. D.; Reed, A. E.; Carpenter, J. E.; Weinhold, F. NBO version 3.1.

(23) Schleyer, P. v. R.; Maerker, C.; Dransfeld, A.; Jiao, H.; Hommes, N. J. R. v. E. *J. Am. Chem. Soc.* **1996**, *118*, 6317.

(24) Wolinski, K.; Hilton, J. F.; Pulay, P. *J. Am. Chem. Soc.* **1990**, *112*, 8251.

(25) (a) Tomasi, J.; Persico, M. *Chem. Rev.* **1994**, *94*, 2027 (b) Cossi, M.; Barone, V.; Cammi, R.; Tomasi, J. *Chem. Phys. Lett.* **1996**, *255*, 327. (c) Mineva, T.; Russo, N.; Sicilia, E. *J. Comput. Chem.* **1998**, *19*, 290.

(26) Barone, V.; Cossi, M.; Tomasi, J. *J. Chem. Phys.* **1997**, *107*, 3210.

(27) Barone, V.; Cossi, M. *J. Phys. Chem. A* **1998**, *102*, 1995.

(28) Schmidt, M. W.; Baldridge, K. K.; Boatz, J. A.; Elbert, S. T.; Gordon, M. S.; Jensen, J. J.; Koseki, S.; Matsunaga, N.; Nguyen, K. A.; Su, S.; Windus, T. L.; Dupuis, M.; Montgomery, J. A. *J. Comput. Chem.* **1993**, *14*, 1347.

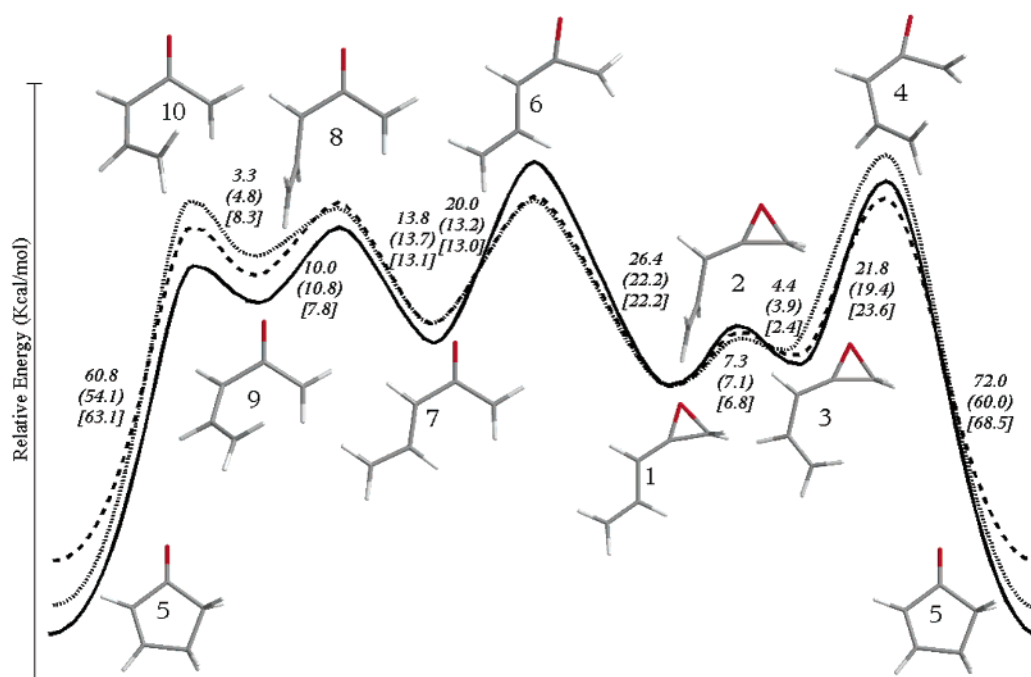


FIGURE 1. Free energy profiles for the rearrangement of **1a** (solid line and stereomodels), **1e** (*anti/in*; dotted line, values in brackets), and **1f** (*anti/in*; dashed line, values in parentheses) computed at 298 K.

TABLE 1. Relative Free Energies (kcal/mol) in the Gas Phase for the Rearrangement of Vinyl Allene Oxides **1a–d**^a

structure ^c	reaction a ^b	reaction b ^b	reaction c	reaction d (syn/out) ^d	reaction d (anti/in) ^d
5	-47.31	-50.3	-45.60	-44.72	-42.05
10	13.47	13.4	17.18	11.33	18.89
9	10.13	10.4	11.41	8.20	13.37
8	20.17	20.7	18.91	19.41	17.76
7	6.33	6.9	4.49	4.39	3.83
6	26.39	27.9	25.65	25.65	25.01
1	0.00	0.0	0.00	0.00	0.00
2	7.27	7.2	6.63	6.92	7.42
3	2.91	3.1	3.80	3.03	2.95
4	24.74	25.2	30.16	24.71	23.88
5	-47.31	-50.3	-45.60	-44.72	-42.05

^a Computed at the B3LYP/6-311++G(3df,2p)//B3LYP/6-31++G(d,p) level of theory. ^b Previous computations at the 6-31G(d) level (ref 12) are shown in *italics*. ^c Even numbering corresponds to transition structures whereas odd numbering corresponds to reactants and products (see Figure 1). ^d For the *syn/out* and *anti/in* descriptors, see Figure 3. Rate-limiting transition states for both mechanisms are indicated in **bold**.

age. The active space includes all the 6 π electrons in the molecule plus the oxygen lone pairs. The orbitals used to construct the active space were obtained from a previous HF/6-311++G(d,p) energy calculation.

Results and Discussion

(a) Parent System 1a. Before embarking on the study of more substituted systems, we confirmed the previous findings¹² that revealed the availability of two competing mechanistic pathways for the rearrangement of vinyl allene oxide **1a** and (*Z*)-propenyl allene oxide **1b** as shown in Scheme 2. Figure 1 shows a diagram depicting the geometries (coordinates for all the computed structures can be found in the Supporting Information) and relative energies of the characterized species in the cyclization of **1a**. Table 1 lists the relative gas-phase free energies at the 6-311++G(3df,2p)//6-31++G(d,p) level of the 10 species **1–10** corresponding to the rearrangement of alkenyl allene oxides **1a** and **1b**,²⁹ along with the values reported by Hess and co-workers at the 6-31G(d) level of theory.¹²

For **1a**, the concerted mechanism involves the cleavage of the oxide terminal bond starting from the *s-cis* conformer **3a** assisted by the concomitant backside attack of the double bond π electrons to form the C–C bond and provide cyclopent-2-en-1-one **5a** via transition structure **4a**. A value of 24.74 kcal/mol was computed for the activation energy of the concerted rearrangement.

The rate-limiting step in the stepwise mechanism is the ring opening of the *s-trans* conformer of vinyl allene oxide **1a** to afford the *s-trans* oxidopentadienyl zwitterion **7a**, and the estimated energy of activation in the gas phase was 26.39 kcal/mol, ca. 1.65 kcal/mol above the energy of TS **4a** (Table 1). Both ring opening and C–O bond rotation are significantly advanced in the transition structure **6a**, which showed 66% of the total bond elongation and 61% of the total bond rotation. Subsequent conformational change produces the nonplanar *s-cis*-oxidopentadienyl zwitterion **9a** from *s-trans*-**7a** via

(29) Only the reactants with the *E* geometry of the allene oxide were considered in this work.

TS **8a**. The conrotatory electrocyclic ring closure of **9a** requires an energy of activation of only 3.34 kcal/mol to place both methylene termini at bond distance and reach TS **10a**, which collapses to the product **5a** in a highly exothermic process.

The frontier molecular orbitals and spin state for the concerted and stepwise mechanisms exhibit several distinct features. Structures with closed-shell configurations were found in the concerted mechanism (from **1** to **5**), despite attempts to force an unrestricted solution to the SCF. The same behavior was found in TS **6**, the only distinctive feature of this structure being the charge separation, remarkably larger than in TS **4**. Upon formation of the oxidopentadienyl zwitterion **7**, a singlet unrestricted wave function was found to represent the electronic ground state of the system (all species from **7** to **10**). Indeed, when the closed-shell solution of the SCF is checked to be a minimum,³⁰ a RHF to UHF instability was found. The instability is due to the breaking of the spin symmetry leading to species with diradical character, but this feature does not noticeably alter their charge distribution (relative to TS **6**).³¹ Hence, the present calculations suggest that the structures in the stepwise pathway are zwitterions with some radical features that might play a role in their chemical behavior (vide infra).

Since TS **4a** was described as a π -bond-assisted back-side epoxide ring opening having S_N2 reaction features, we performed orbital analysis to accurately depict its electronic distribution. Being the allene oxide terminus tetrahedral, no significant rotation of this atom is required to have it engaged in C–C bond formation.³² In fact, the imaginary frequency corresponds to a linear motion of the terminal sp^3 allene oxide carbon toward the rotating sp^2 at the other end of the cyclizing system. The reaction could therefore be considered as monorotatory.³³ NBO analysis²² of TS **4a** is consistent with the breaking C–O bond keeping a considerable contribution of a π bond. Analysis of the electron density³⁴ reveals the existence of a single RCP (ring critical point of the electron density) in the middle of the cyclopentene system, but no RCP was found in the oxacyclopropane ring. The nonexistence of the RCP and, consequently, the absence of a BCP (bond critical point of the electron density) between oxygen and carbon further strengthens the idea of an irregular bond pattern in TS **4a**. On the other hand, even though the concerted pathway proceeds via closed shell stationary structures, a closer look into the mechanism reveals that the statement does not necessarily apply to the entire concerted reaction profile. IRC calculations starting from TS **4a** proved challenging, and a narrow region was found in which the wave function exhibits considerable spin contamination and diradical character. When this RHF to UHF crossover occurs the initial seemingly monorotatory cyclization of **3a** to TS **4a** resembles a disrotatory movement of the

termini carbon atoms and then “changes direction” to afford **5a** by a conrotatory movement.³⁵

The bond-forming event in the stepwise mechanism is the electrocyclic ring closure of an oxidopentadienyl zwitterion intermediate **9a**. By analogy to the Nazarov reaction,^{16,36} which involves a $4\pi e^-$ hydroxypentadienyl cation, the C–C bond formation of **9a** to afford product **5a** through TS **10a** was first viewed³⁷ as an electrocyclic ring closure having aromatic character. Orbital symmetry analysis predicts a conrotatory movements of the termini atoms of **9a**.³⁸ However, examination of the charge distribution in TS **10a** obtained from several population analysis methods suggests an alternative description, namely an intramolecular collapse of radicals. Values of the spin densities extracted from Mulliken and NBO population analysis support this view of the cyclization as the combination of high energy electrons localized at atoms clearly forming two radical systems with enol and allyl character. Atomic charges are also consistent with the diradical nature of TS **10a**, the bond-forming carbons showing partial negative charges due to opposite spin electrons. Values of separate α and β NBO atomic charges are listed in the Supporting Information (Table S5). The cyclizing termini C1 and C5 show localized α and β densities, respectively, and C3 also accumulates β charge accounting for the allyl system C3–C5. A graphical representation of the spin densities for TS **10a** is shown in Figure S1 (Supporting Information). The moderate values of the isotropic magnetic shielding³⁹ along the axis that traverses the center of the forming ring are also consistent with the diradical nature of TS **10a** (see Figure S2 of the Supporting Information).

Due to the significant diradical character exhibited by all the structures along the stepwise pathway, we expected a Bürgi–Dunitz-type approach involving no rotatory motion of the termini atoms toward TS **10a**. Contrary to our expectations, the imaginary frequency is associated with a clear conrotatory movement of the carbon termini in TS **10a**.

Despite the fact that DFT methods provide accurate energies and geometries even with wave functions showing high spin-contamination,⁴⁰ the Kohn–Sham orbitals and single-determinant wave function may not be the most reliable since these systems exhibit a high degree of nondynamical correlation that arises from its intrinsic double configuration nature. The multiconfigurational treatment is one of the best approaches to the exact wave

(35) A somehow related change in rotational motions has been noted in the rearrangement of allene oxides to cyclopropanones (ref 15).

(36) (a) Smith, D. A.; Ulmer, C. W. *Tetrahedron Lett.* **1991**, 32, 725. (b) Smith, D. A.; Ulmer, C. W. *J. Org. Chem.* **1991**, 56, 4444. (c) Smith, D. A.; Ulmer, C. W. *J. Org. Chem.* **1993**, 58, 4118. (d) Smith, D. A.; Ulmer, C. W. *J. Org. Chem.* **1997**, 62, 5110.

(37) A reviewer suggested that these reactions could be better described as pseudopericyclic. Usually, pseudopericyclic reactions are characterized by the absence of rotation in both termini of the reactant and very small energy barriers. In the system under study, the double bond clearly rotates, and barriers are high, which seems to discard the pseudopericyclic nature of the rearrangement.

(38) Woodward, R. B.; Hoffmann, R. *Angew. Chem., Int. Ed. Engl.* **1969**, 81, 797.

(39) NICS values for transition states of concerted reactions typically range from 14 to 24. For comparison, see Figure 3 in: Morao, I.; Lecea, B.; Cossio, F. P. *J. Org. Chem.* **1997**, 62, 7033. See also Tables 3 and 4 in: Cossio, F. P.; Morao, I.; Jiao, H.; Schleyer, P. v. R. *J. Am. Chem. Soc.* **1999**, 121, 6737.

(40) Orlova, G.; Goddard, J. D. *J. Chem. Phys.* **2000**, 112, 10085 and references therein.

(30) Bauernschmitt, R.; Ahlrich, R. *J. Chem. Phys.* **1996**, 22, 9047.

(31) $\langle S^2 \rangle$ values and dipole moments for the gas-phase reactions are provided in the Supporting Information.

(32) For the description of TSs of hydrocarbon pericyclic reactions, see: (a) Houk, K. N.; Li, Y.; Evanseck, J. D. *Angew. Chem., Int. Ed.* **1992**, 31, 682. (b) Houk, K. N.; González, J.; Li, Y. *Acc. Chem. Res.* **1995**, 28, 81.

(33) Fabian, W. M. F.; Kappe, C. O.; Bakulev, V. A. *J. Org. Chem.* **2000**, 65, 47.

(34) Bader, R. F. W. *Atoms in Molecules: A Quantum Theory*; Clarendon Press: Oxford, 1990.

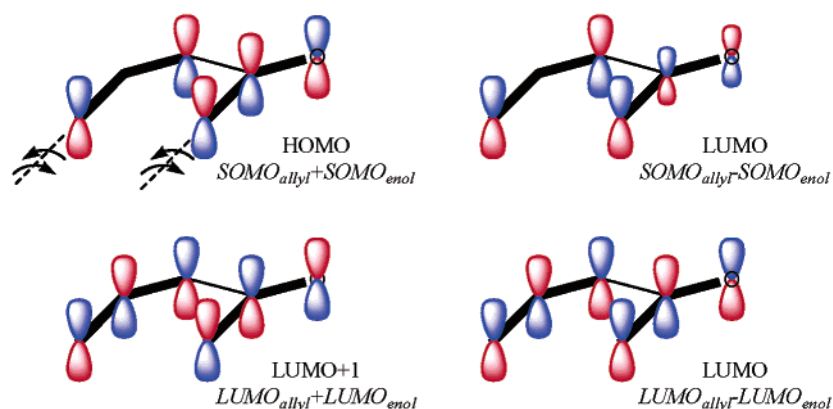
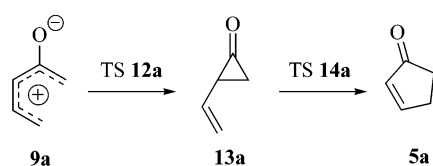


FIGURE 2. Representation of molecular orbitals extracted from CASSCF(10,10) of TS **10a** showing the dissection of the oxidopentadienyl into an allyl and an enol diradical system.

SCHEME 3



function for diradicals. Thus, CASSCF (10,10) calculations were selected to model the electronic features of TS **10a**. This large active space ensures recovery of nondynamic correlation and the natural orbitals obtained become suitable for reactivity analysis. Examination of the frontier π -orbitals obtained from the CASSCF calculation indicates that the electronic system may be split into two fragments, an allyl radical and an enol radical.⁴¹ Four molecular orbitals arise as a result of in-phase and out-of-phase linear combination of these fragments' HOMO and LUMO. This analysis suggests that favorable molecular orbital overlap in the diradical system TS **10a** leads to bond formation to afford **5a** via conrotation (Figure 2).

We also took into consideration a third mechanistic pathway, which starts with the allene oxide to cyclopropanone rearrangement⁴² (**9a** to **13a**) and is then followed by cyclization of **13a** to product **5a** by a vinyl cyclopropanone to cyclopentenone sigmatropic shift (Scheme 3). The oxidopentadienyl (zwitterion or diradical) to cyclopropanone rearrangement takes place through TS **12a**, which lies 11.0 kcal/mol above **9a**. It was then deemed unlikely that this alternative pathway competes with the ring closure of **9a** to **5a** via TS **10a** (cf. 3.3 kcal/mol, Scheme 2). Moreover, attempts to find a concerted path linking **13a** to **5a** proved unsuccessful, even with the more widely employed 6-31G(d) and 6-31+G(d) basis sets, and TS **10a** was instead intercepted.

(b) Vinyl Allene Oxides with a Methyl Substituent (1b–d). As a confirmation of the sensitivity of the system to the steric effects of the substituents, computa-

tions of the *Z*- and *E*-propenyl allene oxides **1b** and **1c** provided opposite outcomes. The energy profile for the concerted rearrangement of the *E* isomer **1c** is in line with that computed for the parent system **1a**; however, the opening of the epoxide via the zwitterionic pathway is 0.74 kcal/mol less costly than that of **1a**, likely due to the stabilization of the carbenium ion in the forming oxidopentadienyl zwitterion by the methyl group. This stabilization contributes to reduce the difference in activation energies between the rate-limiting steps of the mechanistic dichotomy from 1.65 (**1a**) to 0.94 kcal/mol (**1c**) in favor of the concerted path. Values of relative energies are listed in Table 1.

In contrast, although the energy values computed for the rearrangement of the *Z* isomer **1b** reflect the steric effect of the methyl group, this is kinetically significant only in the concerted pathway. The formation of the zwitterionic oxidopentadienyl **7** from *s-trans*-**1** via TS **6** is virtually insensitive to the geometry of the terminal double bond, since the energies of activation for the epoxide ring opening step of the stepwise process are the same, 25.65 kcal/mol, for both isomers **1c** and **1b**. For **1b**, the opening of the epoxide by assistance of the alkene bond starting with the nonplanar *s-cis*-**3b** is disfavored relative to **3a** due to the more severe Me-H steric interactions that raise considerably the energy of TS **4b** (30.16 vs 24.74 kcal/mol for TS **4a**). Therefore, the stepwise path is predicted to be considerably favored (by 4.51 kcal/mol) over the concerted path in the gas phase, a finding in contrast to that previously reported for the rearrangement of *Z*-propenyl allene oxide **1b** at the 6-31G(d) level¹² reporting a 36% lower energy difference between these transition states, thus predicting a more competitive process.

When the tetrahedral carbon of the allene oxide is substituted, as in **1d**, diastereomeric transition structures are possible within each mechanistic path. We have labeled those structures using the *syn/anti* and *out/in* descriptors. *Syn/anti* is meant to describe the formation of the helical TS **4d** toward/away the allene oxide substituent during the *concerted* mechanism. To accurately describe the movement of the allene oxide substituent relative to the epoxide (inside or outside the pentenyl system) in the *stepwise* mechanism, the terms *in/out* were instead chosen.⁴³ The geometrical meaning of these terms can be understood by looking at the *syn/*

(41) See, for example: (a) Davidson, E. R.; Gajewski, J. J. *J. Am. Chem. Soc.* **1997**, *119*, 10543. (b) Houk, K. N.; Nendel, M.; Wiest, O.; Storer, J. W. *J. Am. Chem. Soc.* **1997**, *119*, 10545. (c) Nendel, M.; Sperling, D.; Wiest, O.; Houk, K. N. *J. Org. Chem.* **2000**, *65*, 3259.

(42) (a) Camp, R. L.; Greene, F. D. *J. Am. Chem. Soc.* **1968**, *90*, 7349. (b) Sclove, D. B.; Pazos, J. F.; Camp, R. L.; Greene, F. D. *J. Am. Chem. Soc.* **1970**, *92*, 7488. (c) Sorensen, T. S.; Sun, F. *Can. J. Chem.* **1997**, *75*, 1030. (d) Hess, B. A. *Org. Lett.* **2002**, *4*, 35.

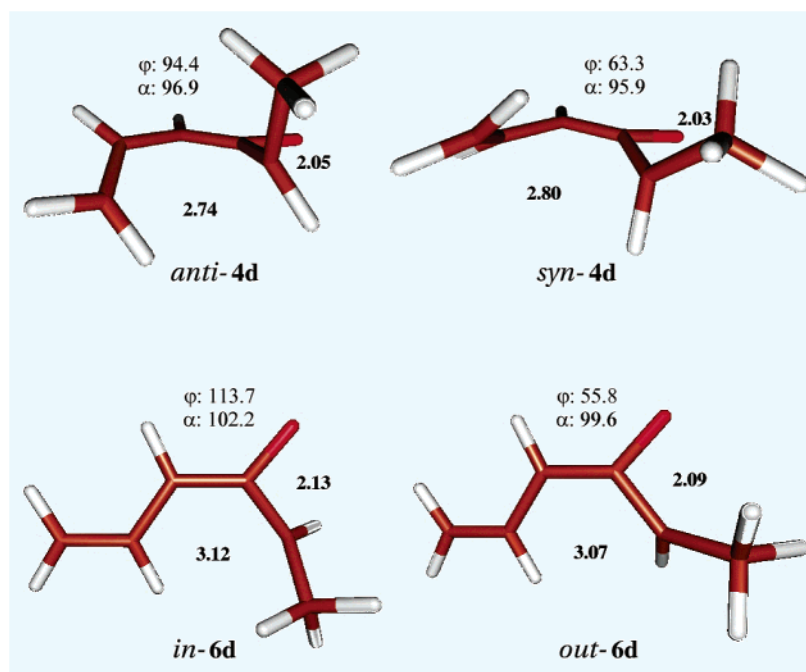


FIGURE 3. Representation of the concerted (top) and zwitterionic (bottom) TSs for the rearrangement of vinyl allene oxide **1d**. Breaking/forming bond distances are shown in boldface. The degree of epoxide breakage is reflected in the values of α (the epoxide OCC_{terminal} bond angle) and φ (the OCC_{terminal}C_{methyl} dihedral angle).⁴³

out and *anti/in* transition structures depicted in Figure 3 for the rearrangement of reactant **1d**.

The harmonic analysis of the concerted TS *anti-4d* reveals an imaginary frequency with an associated motion that leads directly to 5-methylcyclopent-2-en-1-one **5d** (Scheme 2). This frequency involves the translational movement of the epoxide terminus straight toward the π bond and the concomitant rotatory movement of the terminal sp² carbon to improve orbital overlap. On the other hand, although the main component of the imaginary frequency of TS *syn-4d* is also the opening of the epoxide toward the π bond in concert with the rotation of the π bond, the extent of rotation is considerably smaller in this case. The greater advance of the sp³ bond motion toward the other terminus together with the reluctance to rotation of the vinyl bond reduce the steric interaction between the methyl group and the facing vinyl hydrogens in TS *syn-4d*. Nevertheless, TS *syn-4d* is destabilized by 1.09 kcal/mol relative to TS *anti-4d*. Even greater differences in activation energies were found for the alternative stepwise processes through TS *out-6d* and TS *in-6d*. The *out* cleavage of the epoxide ring is more costly (2.19 kcal/mol) than the alternative *in*, in part because of the greater steric interactions between the methyl substituent and its neighboring groups in TS *out-6d*.

The epoxide methyl group stabilizes the oxidopentadienyl zwitterion by hyperconjugation, leading to a significant reduction (up to 3.57 kcal/mol) in the energy of TS *in-6d* of the stepwise process. However, all species along the stepwise pathway past TS *in-6d* are destabilized between 3.09 and 5.42 kcal/mol relative to parent

system. The rate-limiting step becomes now the *s-trans* **7d** to *s-cis* **9d** conversion via TS **8d**. The stabilization of the alternative concerted TS *anti-4d* is smaller (1.95 kcal/mol), and the difference in the activation energies determining the reaction course is reduced to 0.49 kcal/mol, thus both mechanisms showing themselves highly competitive. All species of the *out* stepwise process are stabilized relative to the unsubstituted system. An additional feature of the energy profile for the allene-substituted **1d**, not shared by the parent system or the alkene-substituted **1b** and **1c**, is the similar activation energies computed for the forward and reverse reactions of intermediate **7d**. The modest (0.47 kcal/mol) energy difference between the rate-limiting steps of the mechanisms available to **1d**, together with the reversibility of **7d**, enhance the loss of stereochemical information of the epoxide stereocenter if an enantiopure reactant were used.

(c) Disubstituted Vinyl Allene Oxides **1e** and **1f**.

For systems **1e** and **1f** that combine stereochemical markers at both termini of the vinyl allene oxides, four TSs are likewise possible for each geometric isomer: *syn* and *anti* approaches of the double bond (*E* or *Z* geometry) to the opening epoxide ring in the concerted rearrangement and *out* and *in* motions of the allene methyl group in the formation of the zwitterions along the stepwise mechanism. To complicate the scenario, two diastereomeric products *cis-5e* and *trans-5e* are possible starting from either isomer of the reactant (Scheme 4). If sufficient energy difference between the diastereomeric concerted TSs (*syn/anti*) exists, the rearrangement of **1e** and **1f** along the concerted mechanism could take place torquoselectively to afford either *cis-5e* or *trans-5e* with high diastereoselectivity. If relative configuration is controlled by torquoselectivity, the reaction of enantiopure reactants (note that chiral structures of Scheme 2 and 4 are

(43) Notice that the stereochemical markers *in/out* in this paper are used to describe the movement of the epoxide substituent along the stepwise mechanism, and they are unrelated to the same descriptors used by Houk in his original paper on torquoselectivity.

SCHEME 4

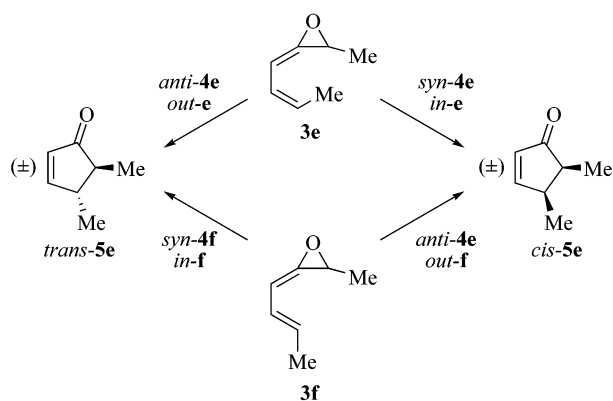


TABLE 2. Relative Free Energies (kcal/mol) in the Gas Phase for the Rearrangement of Dimethyl-Substituted Vinyl Allene Oxides **1e and **1f**^a**

structure ^b	reaction e		reaction f	
	<i>syn/out</i> ^c	<i>anti/in</i> ^c	<i>syn/out</i>	<i>anti/in</i>
5	-38.29	-40.35	-39.45	-37.39
10	15.15	22.74	9.93	16.77
9	9.92	14.42	6.54	11.96
8	16.29	22.27	16.95	22.75
7	2.37	9.14	3.37	9.04
6	24.54	22.18	24.70	22.21
1	0.00	0.00	0.00	0.00
2	6.86	6.86	7.06	7.06
3	3.74	4.50	3.03	3.13
4	28.62	28.12	24.13	22.58
5	-38.29	-40.35	-39.45	-37.39

^a Computed at the B3LYP/6-311++G(3df,2p)//B3LYP/6-31++G(d,p) level of theory. ^b Even numbering corresponds to transition structures whereas odd numbering corresponds to reactants and products (see Figure 1). ^c For the *syn/out* and *anti/in* descriptors, see Figure 3. Rate-limiting transition states for both mechanisms are indicated in **bold**.

racemates) along a highly favored concerted pathway should also proceed enantioselectively affording enantiopure products *cis-5e* or *trans-5e*. On the other hand, the stepwise path, if favoured, encounters planar structures (**7e** and/or **7f**) and consequently the absolute stereochemical information would be lost starting from enantiopure reactants. The conrotatory electrocyclic ring closure of oxidopentadienyl zwitterions **9e** or **9f** would therefore provide the corresponding *cis-5e* or *trans-5e*, respectively, as racemates, as long as the geometry of the intermediates is maintained along the stepwise path.

Table 2 lists the relative energies of the species involved in the rearrangement of doubly substituted models **1e** and **1f**. The computations further confirm and extend the conclusions reached earlier for the singly substituted systems. For the *E* isomer **1f**, TSs **4f** and **8f** for the *anti/in* motion are of lower energy than the alternative *syn/out*. Moreover, the concerted mechanism going through *anti-4f* lies only 0.17 kcal/mol below the stepwise transition state TS **8f** and consequently it is predicted that **1f** will select the *anti* helical transition structure to provide *trans-4,5*-dimethylcyclopent-2-en-1-one **5f** to some extent. A more detailed kinetic treatment which takes into consideration the small energy difference between the rate-limiting steps and the reversibility of the *in* stepwise process in substrates substituted at

the epoxide terminus is provided in the Supporting Information (vide infra).

On the other hand, the stepwise *in* mechanism is the lowest energy path for the rearrangement of the *Z* isomer **1e**. The 1.80 kcal/mol difference of TS *in-10e* relative to TS *out-4e*, the second with the lowest energy, ensures that the stepwise mechanism along TS *in-6e* will be predominantly followed by **1e** to afford *cis-4,5*-dimethylcyclopent-2-en-1-one **5e**. The product *cis-5e* would be a racemate, even if enantiopure **1e** were used. Steric hindrance between the termini atoms increases the energy barriers for both concerted transition states *syn-4e* and *anti-4e* dropping them out of the competitive reaction. This effect can also be observed in reaction **b** where energy barrier for the concerted alternative is 5 kcal/mol higher than in reactions **a** (unsubstituted) and **c** (*E*-substituted).

Consistent with the findings on system **1d**, substitution at the epoxide terminus produces a systematic stabilization of all the species along the *out* stepwise mechanism and an opposite destabilization along the *in* alternative in both **1e** and **1f**, with the exception of TS *out-10e*. As a consequence, the sterically more hindered TS *in-10e* (8.3 kcal/mol) of the zwitterionic pathway is the species with the highest energy increase relative to the parent system (3.3 kcal/mol). Due to this steric destabilization, the electrocyclic ring closure of *in-9e* to *cis-5e* becomes the rate-limiting step.

The isomerization of the oxidopentadienyl zwitterions **7** and **9** by double-bond rotation was also examined. An energy value of 24.9 kcal/mol was computed for the rotational TS exchanging the substituents of the terminal double bond in **7a**. It was then surmised that double bond isomerization or scrambling are unlikely and oxidopentadienyl intermediates (**7b**, **7c**, **7e**, **7f**) preserve their stereochemical information along the reaction coordinate.

Observation of the highly competitive profiles in gas phase (Tables 1 and 2; Figure 1 shows the energy profiles of **1e** and **1f** in comparison with the parent system) led to the conclusion that a reasonable prediction for the product distribution of the epoxide-substituted vinyl allene oxide cannot merely be based on a comparison of activation energies of the mechanistic duality. Kinetic simulations were then performed with the CKS⁴⁴ package in order to better address the problem of competitive processes with comparable activation barriers. Stochastic simulations for the systems under study are based on the algorithm published by Gillespie,⁴⁵ which is known to provide accurate results, close to those obtained by integration of the coupled differential equations. These data and further discussion on the implications of the energy profile in the kinetics of the reaction can be found in the Supporting Information.

Solvent Effects. Determination of solvent effects using the PCM²⁵ (or CPCM²⁷) methods with CH₂Cl₂ led to very small differences in the energetics of the TSs for the rate-limiting steps (see Table 3) of model system **1a**

(44) The Chemical Kinetics Simulator program package, including supporting documentation, is available for a no-cost license from IBM Almaden Research Center at www.almaden.ibm.com/st/computational_science/ck/msim/.

(45) Gillespie, D. T. *J. Comput. Phys.* **1976**, *22*, 403.

TABLE 3. Relative Free Energies (kcal/mol) for the Rearrangement of Vinyl Allene Oxides 1a–f in Solvent (PCM)^a

structure ^b	reaction a	reaction b	reaction c	reaction d		reaction e		reaction f	
				(<i>syn/out</i>) ^c	(<i>anti/in</i>) ^c	(<i>syn/out</i>)	(<i>anti/in</i>)	(<i>syn/out</i>)	(<i>anti/in</i>)
dichloromethane									
5	-49.75	-46.67	-45.66	-43.91	-43.91	-39.16	-40.96	-40.08	-38.28
10	10.53	14.89	8.79	8.93	15.44	12.39	20.65	6.81	13.56
9	8.51	9.69	6.44	6.68	11.61	8.48	12.12	4.68	9.51
8	18.62	16.19	18.17	15.94	20.97	14.89	20.64	15.24	20.66
7	4.39	2.79	2.27	1.11	8.37	-0.50	6.87	0.35	5.98
6	25.72	25.00	25.03	22.91	20.70	22.64	20.23	22.92	20.35
1	0.00	0.00	0.00	0.00	0.00	0.00	0.00	0.00	0.00
2	7.96	6.81	7.04	7.86	7.86	7.54	7.54	7.29	7.29
3	3.07	4.06	3.30	3.14	2.64	4.79	4.58	3.07	3.57
4	23.83	29.30	24.26	22.35	21.23	27.08	26.60	22.89	21.19
5	-49.75	-46.67	-45.66	-43.91	-43.91	-39.16	-40.96	-40.08	-38.28
water									
5	-50.37	-45.79	-44.6	-43.7	-43.7	-37.6	-39.96	-39.53	-37.17
10	8.61	13.06	9.08	7.57	13	9.75	19.28	4.28	10.81
9	7.55	7.89	6.17	5.6	10.86	8.85	10.95	4.88	7.22
8	17.46	15.89	17.77	15.04	20.34	15.03	20.14	15.07	19.75
7	3.16	2.67	1.7	-0.98	7.74	-2.7	7.34	-1.78	3.58
6	25.58	25.23	25.53	21.34	19.03	21.9	20.05	22.19	20.39
1	0.00	0.00	0.00	0.00	0.00	0.00	0.00	0.00	0.00
2	8.37	6.6	7.46	8.45	8.45	8.32	8.32	7.34	7.34
3	3.06	4.12	3.11	3.01	2.48	5	4.89	2.27	3.15
4	23.69	29.9	25.04	21.3	20.11	26.59	25.68	22.12	20.59
5	-50.37	-45.79	-44.6	-43.7	-43.7	-37.6	-39.96	-39.53	-37.17

^a Computed at the B3LYP/6-311++G(3df,2p)//B3LYP/6-31++G(d,p) level of theory. ^b Even numbering corresponds to transition structures whereas odd numbering corresponds to reactants and products (see Figure 1). ^c For the *syn/out* and *anti/in* descriptors, see Figure 3. Rate-limiting transition states for both mechanisms are indicated in **bold**. Similar results were obtained by means of the COSMO model (Supporting Information).

relative to the gas phase.⁴⁶ To provide comparison, the free energy of solvation was also calculated with the water parameters to take into account limit effects onto the reaction profile and the nature of the wave function due to solvation with a charge stabilizing solvent. Calculations in water showed only slight differences relative to dichloromethane (Table 3). Both TS **4a** and TS **6a** become stabilized (by 1.07 and 0.67 kcal/mol, respectively) in the presence of solvent. The stabilization is kinetically insignificant along the concerted pathway. The extent of stabilization is greater for the late intermediates in the stepwise mechanism, ranging from 1.5 kcal/mol for **7a** and **8a** to 3 kcal/mol for the bond-forming TS **10a** (precisely the trend observed for the dipole moments of the different species³¹). As was the case for the steric effects, the effect of the solvent in the zwitterionic pathway is a late effect and the reduction in activation energies for the rate-limiting steps is moderate and does not alter the mechanistic discussion.

Similar considerations apply to the rearrangement of the propenyl allene oxides *Z* and *E*, **1b** and **1c**, respectively, in the presence of CH₂Cl₂ (Table 3). However, substitution at the epoxide carbon as in system **1d** showed from two to three times greater solvent stabilization of the relevant TSs *anti-4d* and *in-8d* than the vinyl/propenyl analogues **1a–c**, particularly so for the zwitterionic TS *in* (ca. 2.5 kcal/mol; ca. 1.0 kcal/mol more than the corresponding concerted *anti*). The reversal in activa-

tion energies relative to gas phase for these steps is not found in water.

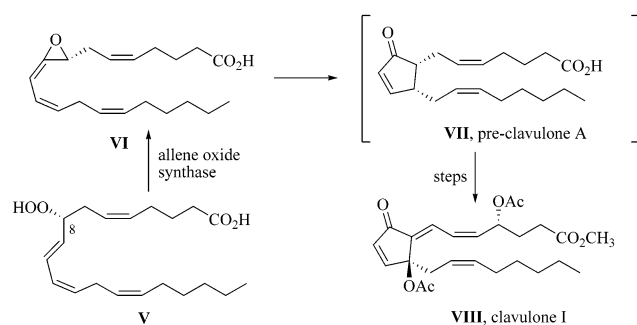
The effect of solvent (PCM) in the activation energies determining the mechanistic fate of the doubly substituted vinyl allene oxides **1e** and **1f** are an extension of that described for the unsubstituted and singly substituted analogues. The extent of stabilization for the TSs of the *E* isomer **1f** ranges from 1.39 (*anti-4f*) to 2.09 kcal/mol (*in-8f*). For these systems, although the effect on product distribution is small since the main features observed in the gas-phase profile are maintained in solvent, the preferred *anti-in* mechanisms are still highly competitive and lay 2–2.5 kcal/mol below the disfavored *syn-out* alternative. Transition state stabilization of the same magnitude are computed for the *Z* isomer **1e**: for the *anti* concerted and *in* stepwise mechanisms, the TSs are lowered by 1.52 kcal/mol (*anti-4e*) and by 2.09 kcal/mol (*in-8e*), respectively, in the presence of solvent. In line with the results in vacuo, the bond forming step (*in-9e* to **5e**) is now rate limiting (20.65 kcal/mol). It should lead to a racemic *cis*-4,5-dimethylcyclopent-2-en-1-one via TSs **10e** which has two enantiomeric conrotatory motions allowed by the Woodward–Hoffmann rules.

Conclusions

To summarize, two distinct competing mechanistic pathways have been characterized for the rearrangement of vinyl allene oxides²⁹ to cyclopent-2-en-1-ones. The concerted transition structure can be depicted as a monorotatory ring closure with concomitant epoxide ring opening. It starts from the less stable conformer *s-cis* **3** and was found to have a lower energy of activation for the parent system **3a** and for analogues with *E*-methyl-substituted double bond **1c**. The bond-forming step of the

(46) For other publications describing small solvent effects in reactions proceeding through zwitterionic transition states or intermediates, see: (a) Assfeld, X.; Ruiz-López, M. F.; González, J.; López, R.; Sordo, T. L. *J. Comput. Chem.* **1994**, *15*, 597. (b) López, R.; Ruiz-López, M. F.; Rinaldi, D.; Sordo, T. L. *J. Phys. Chem.* **1996**, *100*, 0. (c) Lecea, B.; Arrieta, A.; Arrastia, I.; Cossío, F. P. *J. Org. Chem.* **1998**, *63*, 5216. (d) Zhou, C.; Birney, D. M. *J. Am. Chem. Soc.* **2002**, *124*, 5231.

SCHEME 5



stepwise mechanism is a conrotatory electrocyclic ring closure of planar *s-cis*-oxidopentadienyl zwitterionic species. NBO analysis is also consistent with an alternative view of the cyclization as a combination of two radicals having allyl and enol characteristics. The energy of activation for the stepwise mechanism is clearly lower than for the concerted pathway for methyl substituted double bonds with *Z* geometry **1b**. The substitution at the epoxide (**1d**, **1e**, **1f**) induces stabilization of the first transition states found along each manifold. However, energies of all intermediates and transition structures along the *out* stepwise pathways are, in general, stabilized whereas those of the *in* alternative are destabilized relative to the parent system. As a consequence, rate-limiting steps lay further from the epoxide opening step in the reaction coordinate of the stepwise pathway. Derivatives **1d** and **1f** show a high competition between the two favored alternatives, *anti*-concerted and *in*-stepwise. For the *E*-disubstituted system **1f**, diastereoselectivity could be expected to some extent, but enantioselectivity is not possible since a considerable amount of molecules yielding the product in a concerted fashion have previously broken the epoxide to form the planar intermediate *in*-**7f**. As in **1b**, analogue **1e** featuring substituents at the epoxide and double bond of *Z* geometry, follows a stepwise pathway in which the methyl group describes an *in* motion toward the pentadienyl system to reach TS **6e** eventually yielding *cis*-**5e**.

Solvent effects do not alter the mechanistic dichotomy, and the changes in activation energies with or without solvent are modest in most cases. Despite the solvent effects upon energies of activation being fairly small, as long as the energy differences between the concerted and stepwise mechanisms for several of the systems under study are insignificant, slight changes promoted by the solvent stabilization can dramatically modify the energy profile and therefore the product distribution, such as in reactions **d** and **f**.

In addition to the plant metabolites, other cyclopent-2-en-1-ones are biosynthesized in soft corals by the lipoxygenase pathway, among them the cyclic fatty acid clavulones (represented by clavulone I, **VIII**, in Scheme 5) and the punaglandins. Despite the functional analogies between the corresponding enzymes, the lipid hydroperoxide substrates for plants and animals have the opposite configuration (13*S* in **I** and 8*R* in **V**).⁵

The vinyl allene oxides intermediates in the biogenesis of **IV** and **VIII** are structurally related to the truncated

system **1e** studied here. Vinyl allene oxides **II** and **VI** differ, among other features, in the absolute configuration of the chiral oxide carbon. They are enzymatically converted into *cis*-**III** and *cis*-**VII**, having opposite absolute configuration of the disubstituted cyclopent-2-en-1-one ring. This outcome would require that the enzyme display opposite enantiofacial torquoselectivity in the electrocyclic ring closure of the putative oxidopentadienyl zwitterions similar to **9e**. In other words, if a stepwise mechanism is operating in the biosynthesis of plants and marine invertebrate cyclopentenones from the vinyl allene oxide with *Z* geometry, the enzyme active site must force the oxidopentadienyl zwitterions to follow an enantiofacial conrotation of opposite sense, i.e., a enantiofacial torquoselective movement (the only possible for ring closure of achiral polyenes) of the termini of the planar intermediate to afford enantiopure *cis*-4,5-disubstituted cyclopent-2-en-1-ones, perhaps by shielding a face of the *s-cis*-oxidopentadienyl zwitterions in the chiral nonracemic active site environment. The enzyme binding site provides a variety of rate-accelerating effects,⁴⁷ namely catalysis of the epoxide ring opening, electrostatic effects, H-bonding, steric hindrance to bond rotations, and ground-state stabilization of the less-stable conformers, which might even divert the substrates along the computationally disfavored concerted pathways (or enforce a chameleonic mechanism having features of the stepwise and concerted). The influence of each effect on the stabilization of the relevant TS cannot be entirely predicted in the absence of the tridimensional structure of the enzyme/substrate complex. The recent cloning of the allene oxide cyclase from potato⁷ raises hopes that successful structural determination may form the basis for more in-depth mechanistic studies of the enzymatic reaction. It is the hope that this synergy between theory and experiment will afford penetrating new insights into the molecular mechanisms of biocatalysis.

Acknowledgment. We thank the Spanish Ministerio de Educación, Cultura y Deportes (FPU Fellowships to C.S. and O.N.), the European Union (Grant No. QOLK-3 2002-02029), the Spanish Ministerio de Ciencia y Tecnología (Grant No. SAF01-3288), and Xunta de Galicia (Grant No. PGIDIT02PXIC30108PN) for financial support and Centro de Supercomputación de Galicia (CESGA) and the Minnesota Supercomputing Institute for allocation of computational time. We are indebted to Profs. Cossío and Ugalde (UPV/EHU) for their hospitality, guidance, and fruitful discussions during summer stays of O.N. and C.S. at UPV. D.Y. is grateful for financial support provided by the National Institutes of Health (Grant No. 1R01-GM62248-01A1).

Supporting Information Available: Cartesian coordinates for all the optimized structures, dipole moments, S^2 values, and COSMO energies for water and dichloromethane; NBO charges, representation of the spin density, and NICS values in TS **10a**; further description of the kinetic simulations. This material is available free of charge via the Internet at <http://pubs.acs.org>.

JO049620Z

(47) García-Viloca, M.; Gao, J.; Karplus, M.; Truhlar, D. G. *Science* **2004**, *303*, 186.